



The Unsteady Micropolar Fluid Flow Past A Sliced Sphere

Basuki Widodo and Rita Ayu Ningtyas

Departement of Mathematics, Institut Teknologi Sepuluh Nopember, Surabaya 60111, Indonesia

Abstract : We consider unsteady micropolar fluid flow pasta sliced sphere. We further develop dimensional governing equations. These equations are obtained from conservation of mass and conservation of momentum equations. We further convert the dimensional governing equations into non-dimensional equations by using non-dimensional variables. Further, the non-dimensional equations are reduced to become non-linear differential equation. The non-linear differential equations are solved by using finite difference method with Keller-box scheme. Numerical results show that the characteristic of unsteady micro-polar fluid on boundary layer flow past a sliced sphere for the velocity profile increases in strong and weak concentrations. When a sliced angle value increases then the velocity profile will increase. The micro-rotation profile increases in strong concentration. However, when the sliced angle increases then the micro-rotation profile will decrease. The micro-rotation profile decreases in weak concentrations. However, then the micro-rotation profile will increase when the sliced angle increases.

Keywords: boundary layer, Keller-Box, unsteady micro polar fluid

1. Introduction

The micropolar fluids proposed by Eringen (1965), are theoretically represent that the fluid contains rigid randomly oriented particles suspended in viscous medium, which have an essential micromotion in rotation. There are many researches consider viscous and micropolar fluid flow that can conduct magnetic field in different geometries, such as flat plate, circular cylinder and a solid sphere. (Mohamed et al, 2016; Mohammad et al, 2014; Widodo et al, 2015a, 2015b, 2016a and 2016b). This paperis interested to investigate micropolar fluid past a sliced sphere. This paper will be discussed about unsteady micropolar fluid flow on boundary layer past a sliced sphere, which focus in front and at a stagnation point, i.e. $x = 0^\circ$. Physical coordinate for the micropolar fluid flow past a sliced sphere is shown in Figure 1.

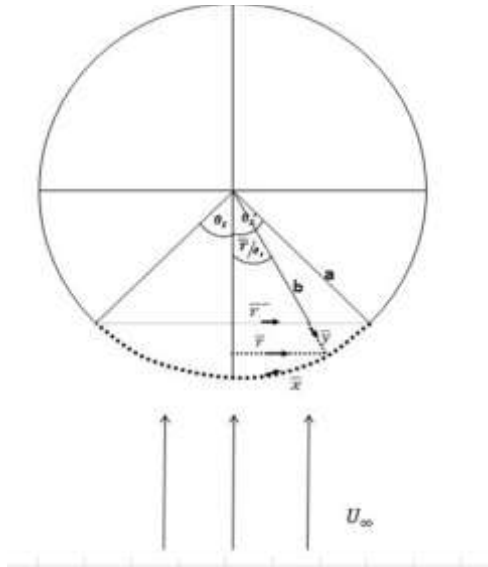


Figure 1. Physical model and coordinate system of a sliced sphere

2. Governing Equations

In this section, we consider mathematical modeling of a micropolar fluid flow. Governing equations for unsteady micropolar fluid flowpast a sliced sphere are from principle of conservations, i.e.conservations of mass and conservation of momentum. The principle of mass conservation states that the sum of the outflow and accumulations must be zero. We obtain the continuity equation, i.e.

$$\nabla \cdot \mathbf{u} = 0 \tag{1}$$

with velocity of fluid is $\mathbf{u} = (u, v, 0)$ and using incompressible micropolar fluid. Further, the principle of conservation of momentum is based on Newton second law of motion. The Newton second law of motions states that the rate of change of momentum in the body equals to the sum of forces applied to the body. We obtain linier momentum equation and it is presented by

$$\rho \left(\frac{\partial \mathbf{u}}{\partial t} + (\mathbf{u} \cdot \nabla) \mathbf{u} \right) = -\nabla p + (\mu + \kappa) \nabla^2 \mathbf{u} + \kappa (\nabla \times \mathbf{N}) - \sigma B_0^2 \mathbf{u} \tag{2}$$

In addition, an angular momentum is represented by

$$\rho j \left(\frac{\partial \mathbf{N}}{\partial t} + \mathbf{N} \cdot \nabla \right) = \gamma \nabla^2 \mathbf{N} + \kappa (-2\mathbf{N} + \nabla \times \mathbf{u}) \tag{3}$$

Equations (1), (2) and (3) can be written by

$$\rho \left(\frac{\partial \bar{u}}{\partial x} + \frac{\partial \bar{v}}{\partial y} \right) = 0 \tag{4}$$

$$\rho \left(\frac{\partial \bar{v}}{\partial t} + \bar{u} \frac{\partial \bar{v}}{\partial x} + \bar{v} \frac{\partial \bar{v}}{\partial y} \right) = -\frac{\partial \bar{p}}{\partial x} + (\mu + \kappa) \left(\frac{\partial^2 \bar{v}}{\partial x^2} + \frac{\partial^2 \bar{v}}{\partial y^2} \right) + \kappa \frac{\partial \bar{N}}{\partial x} - \sigma B_0^2 \bar{v} \tag{5}$$

$$\rho \left(\frac{\partial \bar{u}}{\partial t} + \bar{u} \frac{\partial \bar{u}}{\partial x} + \bar{v} \frac{\partial \bar{u}}{\partial y} \right) = -\frac{\partial \bar{p}}{\partial x} + (\mu + \kappa) \left(\frac{\partial^2 \bar{u}}{\partial x^2} + \frac{\partial^2 \bar{u}}{\partial y^2} \right) + \kappa \frac{\partial \bar{N}}{\partial y} - \sigma B_0^2 \bar{u} \tag{6}$$

$$\rho j \left(\frac{\partial \bar{N}}{\partial t} + \bar{u} \frac{\partial \bar{N}}{\partial x} + \bar{v} \frac{\partial \bar{N}}{\partial y} \right) = \gamma \left(\frac{\partial^2 \bar{N}}{\partial x^2} + \frac{\partial^2 \bar{N}}{\partial y^2} \right) + \kappa \left(-2\bar{N} + \frac{\partial \bar{u}}{\partial y} - \frac{\partial \bar{v}}{\partial x} \right) \tag{7}$$

The basic equations of boundary layer are further transformed into a non-dimensional form. We therefore introduce the following non-dimensional variables, i.e.

$$\begin{aligned}
 M &= \frac{\sigma B_0^2 a}{\rho U_\infty} & K &= \frac{\kappa}{\mu} & N &= Re^{-1/2} \frac{a\bar{N}}{U_\infty} \\
 y &= Re^{1/2} \frac{\bar{y}}{a} & x &= \frac{\bar{x}}{a} & u &= \frac{\bar{u}}{U_\infty} \\
 v &= Re^{1/2} \frac{\bar{v}}{U_\infty} & t &= \frac{U_\infty \bar{t}}{a} & p &= \frac{\bar{p}}{\rho U_\infty^2}
 \end{aligned}$$

By using these the non-dimensional variables and substituting into equation (4), (5), (6) and (7), we obtain non-dimensional governing equations as follows,

$$\frac{\partial u}{\partial x} + \frac{\partial v}{\partial y} = 0 \tag{8}$$

$$\frac{\partial u}{\partial t} + u \frac{\partial u}{\partial x} + v \frac{\partial u}{\partial y} = -\frac{\partial p}{\partial x} + \frac{(1+K)}{Re} \frac{\partial^2 u}{\partial x^2} + (1+K) \frac{\partial^2 u}{\partial y^2} + K \frac{\partial N}{\partial y} - Mu \tag{9}$$

$$\frac{1}{Re} \left(\frac{\partial v}{\partial t} + u \frac{\partial v}{\partial x} + v \frac{\partial v}{\partial y} \right) = -\frac{\partial p}{\partial y} + \frac{(1+K)}{Re^2} \frac{\partial^2 v}{\partial x^2} + (1+K) \frac{\partial^2 v}{\partial y^2} + \frac{K}{Re} \frac{\partial N}{\partial x} - \frac{M}{Re} v \tag{10}$$

$$\frac{\partial N}{\partial t} + u \frac{\partial N}{\partial x} + v \frac{\partial N}{\partial y} = (1+K/2) \left(\frac{1}{Re} \frac{\partial^2 N}{\partial x^2} + \frac{\partial^2 N}{\partial y^2} \right) - K \left(2N + \frac{\partial u}{\partial y} - \frac{1}{Re} \frac{\partial v}{\partial x} \right) \tag{11}$$

Using boundary layer approximation, where the Reynolds number $Re \rightarrow \infty$ so $\frac{1}{Re} = 0$. And then we introduce stream function, ψ , we define the velocity of the fluid in the direction of the x-axis and the y-axis, i.e.

$$u = \frac{1}{r} \frac{\partial \psi}{\partial y} \qquad v = -\frac{1}{r} \frac{\partial \psi}{\partial x}$$

We further have new governing equations, namely

$$\frac{\partial^2 \psi}{\partial x \partial y} = \frac{\partial^2 \psi}{\partial x \partial y} \tag{12}$$

$$\frac{1}{r} \frac{\partial^2 \psi}{\partial y \partial t} + \frac{1}{r} \frac{\partial \psi}{\partial y} \frac{\partial^2 \psi}{\partial x \partial y} - \frac{1}{r^3} \frac{d}{dx} \left(\frac{\partial \psi}{\partial y} \right)^2 - \frac{1}{r^3} \frac{\partial \psi}{\partial x} \frac{\partial^2 \psi}{\partial y^2} \tag{13}$$

$$= u_e \frac{du_e}{dx} + (1+K) \frac{1}{r} \frac{\partial^3 \psi}{\partial y^3} + K \frac{\partial N}{\partial y} + M \left(u_e - \frac{1}{r} \frac{\partial \psi}{\partial y} \right)$$

$$\frac{\partial N}{\partial t} + \frac{1}{r} \frac{\partial \psi}{\partial y} \frac{\partial N}{\partial x} - \frac{1}{r} \frac{\partial \psi}{\partial x} \frac{\partial N}{\partial y} = \left(1 + \frac{K}{2} \right) \frac{\partial^2 N}{\partial y^2} - K \left(2N + \frac{1}{r} \frac{\partial^2 \psi}{\partial y^2} \right) \tag{14}$$

Using similarity variables, i.e. $\psi = t^{\frac{1}{2}} u_e(x) r(x) f(x, \eta, t)$, $\eta = \frac{y}{t^{1/2}}$, $N = t^{1/2} u_e(x) h(x, \eta, t)$ and substituting $\frac{du_e}{dx} = \frac{3}{2 \cos \theta_s}$ we obtain equation such as,

$$(1+K) \frac{\partial^3 f}{\partial \eta^3} + \frac{\eta}{2} \frac{\partial^2 \eta}{\partial \eta^2} + \frac{3}{2 \cos \theta_s} t \left[1 - \left(\frac{\partial f}{\partial \eta} \right)^2 + f \frac{\partial^2 f}{\partial \eta^2} \right] + K \frac{\partial h}{\partial y} + Mt \left(1 - \frac{\partial f}{\partial \eta} \right) = t \frac{\partial^2 f}{\partial \eta \partial t} \tag{15}$$

$$(1+K/2) \frac{\partial^2 h}{\partial \eta^2} + \frac{\eta}{2} \frac{\partial h}{\partial \eta} + \frac{1}{2} h + \frac{3}{2 \cos \theta_s} t \left(f \frac{\partial h}{\partial \eta} - h \frac{\partial f}{\partial \eta} \right) = t \frac{\partial h}{\partial t} + tK \left(2h + \frac{\partial^2 h}{\partial \eta^2} \right) \tag{16}$$

With boundary conditions are

$$t < 0: f = \frac{df}{d\eta} = h = 0 \text{ for any } x, \eta$$

$$t \geq 0: f = \frac{df}{d\eta} = 0, h = -n \frac{\partial^2 f}{\partial \eta^2}, \text{ at } \eta = 0$$

$$\frac{df}{d\eta} = 1, h = 0, \text{ as } \eta \rightarrow \infty$$

In this paper, we solve the problems numerically using Keller-Box method. The method involves the following four steps:

- a. Reduce the transformed equations to a first order system.
- b. Write the difference equations using central differences.
- c. Taking Linearization of the resulting algebraic equations by Newton method and write them into matrix vector form.
- d. Solve the linear system by the block tridiagonal eliminations technique.

3. Result and Discussion

For various of sliced angles *i.e.* ($\theta_s = 15^\circ, 30^\circ, 45^\circ, 53^\circ, 65^\circ, 70^\circ, 80^\circ, 89^\circ$), magnetic parameter ($M = 1$), material parameter ($K = 1$) at $n = 0$ and $n = 0.5$ in which n is a constant and $0 \leq n \leq 1$. The value $n = 0$ represents fully concentrated particle flows, in which the particle density is sufficiently great and those microelements close to the wall are unable to rotate or called as strong concentrations of microelements. In case when corresponding to $n = 0.5$ results in the vanishing of antisymmetric part of the stress tensor and represents weak concentrations of microelements. We further take some numerical simulation by taking some variation of those parameters. We obtain the figures as follows.

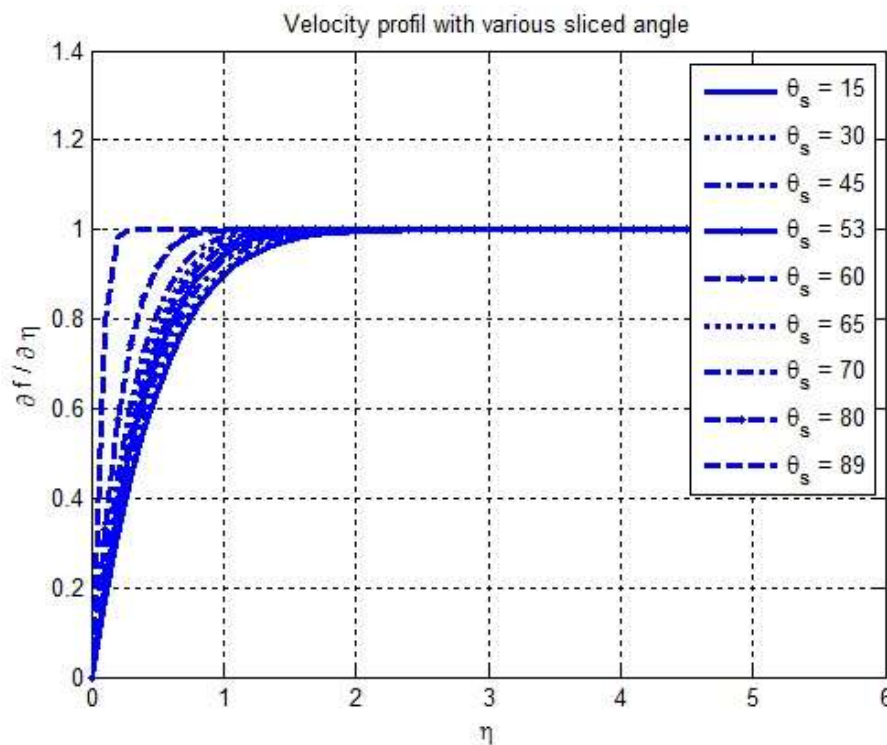


Figure 2. Velocity profile for various θ_s , $K = 1$ and $n = 0$, in front and at the lower stagnation point.

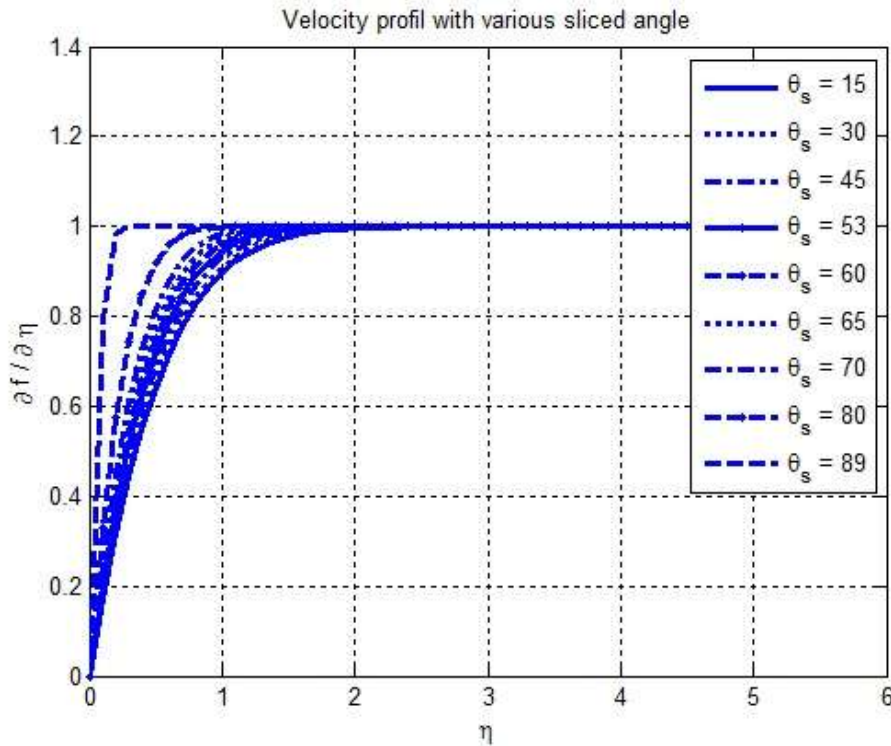


Figure 3. Velocity profile for various θ_s , $K = 1$, and $n = 0.5$, in front and at the lower stagnation point.

Figure 2 and Figure 3 illustrate the velocity profile of unsteady micropolar fluid flow past a sliced sphere at $n = 0$ and $n = 0.5$ with various sliced angle. Results show that by increasing the value of sliced angle result the rising velocity profile of a micropolar fluid. We further to investigate the mirorotation profile when we put some various the sliced angles. We obtain some results as follows,

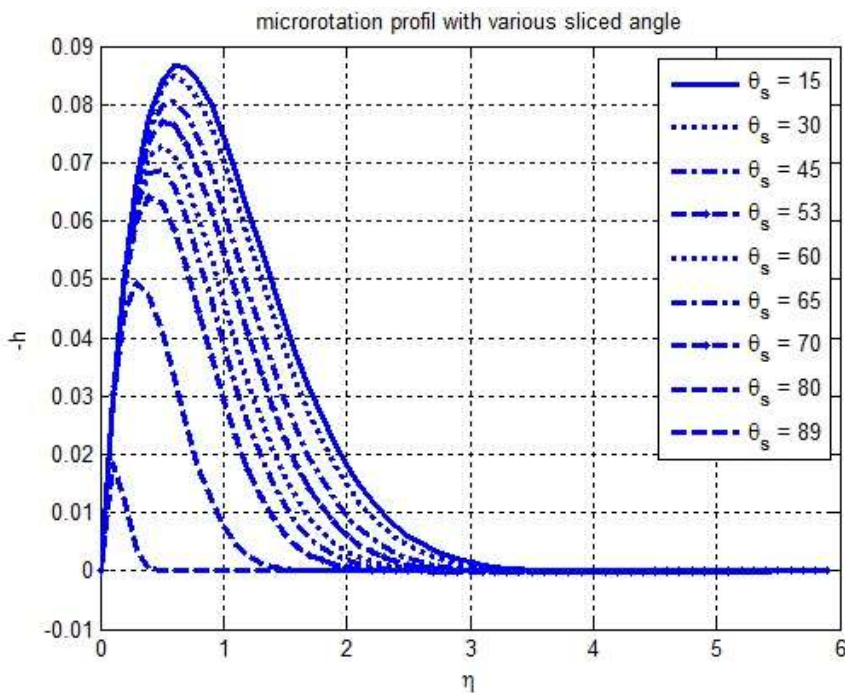


Figure 4. Microrotation profile for various θ_s , $K = 1$, and $n = 0$, in front and at the lower stagnation point.

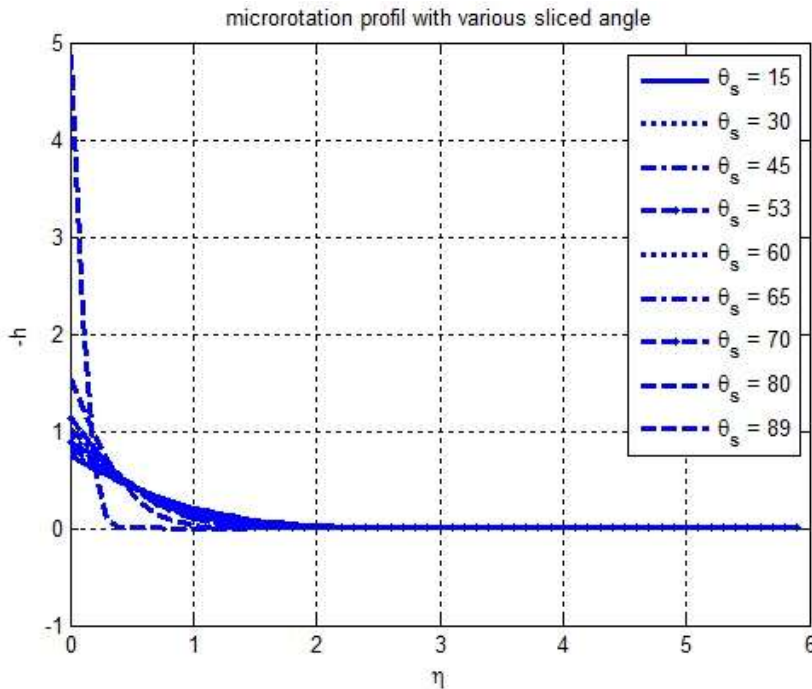


Figure 5. Microrotation profile for various $\theta_s, K = 1$, $d n = 0.5$, in front and at the lower stagnation point.

Figure 4 and Figure 5 show microrotation profiles for various sliced angle of unsteady micropolar fluid flow past a sliced sphere at $n = 0$ and $n = 0.5$. When $n = 0.5$ microrotations profile decrease and when $n = 0$ microrotations profile increase. In these simulations when increasing value of sliced angle in $n = 0.5$ it will increase microrotations profile. However, when increasing value of sliced angle in $n = 0$ it will decrease microrotations profile.

4. Conclusions

The characteristic of unsteady micropolar fluid on boundary layer flow past a sliced sphere for velocity profile increases in strong and weak concentrations. When a sliced angle value increases then the velocity profile will increase. The micro-rotation profile increases in strong concentration. However, when the sliced angle increases then the micro-rotation profile will decrease. The micro-rotation profile decreases in weak concentrations. However, then the micro-rotation profile will increase when the sliced angle increases.

2010 Mathematics Subject Classification: 76A05, 76M20, 76W05

References

1. Erigen, A.C., (1965), Theory of micropolar fluids, Journal of mathematics and Mechanics 16 1-18.
2. Mohamed, M.K.A., Salleh, M.Z., Husanan, A., Sarif, N.M., Noar, N.A.Z., Ishak, A. and Widodo, B., (2016), Mathematical Model Of Free Convection Boundary Layer Flow On Solid Sphere With Viscous Dissipation and Thermal Radiation, International Journal Of Computing Science and Applied Mathematics, Vol.2(2).
3. Mohammad, N. F., (2014), Unsteady Magnetohydrodynamics Convective Boundary Layer Flow Past A Sphere In Viscous and Micropolar Fluids, Universiti Technology Malaysia, Malaysia.
4. Widodo, B., Anggriani, I., and Imron, C., (2015a) The Characterization of Boundary Layer Flow in The Magnetohydrodynamics Micropolar Fluid Past a Solid Sphere, International Conference on Science and innovative Engineering (ICSIE), Kuala Lumpur, Malaysia, 16 Oktober 2015.
5. Widodo, B., Khalimah, D.A., Zainal, F. D. S, and Imron, C., (2015b), The Effect of Prandtl Number and Magnetic Parameters on Unsteady Magnetohydrodynamics Forced Convection Boundary Layer Flow of

- a Viscous Fluid Past A Sphere, International Conference on Science and innovative Engineering (ICSIE), Kuala Lumpur, Malaysia, 16 Oktober 2015.
6. Widodo, B., Anggriani, I., Khalimah, D.A., Zainal, F.D.S., and Imron, (2016a), Unsteady Boundary Layer Magnetohydrodynamics In Micropolar Fluid Past A Sphere, Far East Journal of Mathematics Science (FJMS), Vol. 100(2): 291-299.
 7. Widodo, B., Imron, C., Asiyah, N., Siswono, G.O., Rahayuningsih, T., Purbandini., (2016b), Viscoelastics Fluid Flow Pass A Porous Circular Cylinder When The Magnetic Field Included, Far East Journal of Mathematics Science (FJMS), Vol. 99(2):173-186.
